Microbiome–host systems interactions: Protective effects of propionate upon the blood–brain barrier

Lesley Hoyles[1]*, Tom Snelling[1], Umm-Kulthum Umlai[1], Jeremy K. Nicholson[1], Simon R. Carding[2, 3], Robert C. Glen[1, 4] & Simon McArthur[5]*

[1]Division of Computational and Systems Medicine, Department of Surgery and Cancer, Imperial College London, UK

[2]Norwich Medical School, University of East Anglia, UK

[3]The Gut Health and Food Safety Research Programme, The Quadram Institute, Norwich Research Park, Norwich, UK

[4]Centre for Molecular Informatics, Department of Chemistry, University of Cambridge, Cambridge, UK

[5]Institute of Dentistry, Barts & the London School of Medicine & Dentistry, Blizard Institute, Queen Mary University of London, London, UK

***Corresponding authors:** Lesley Hoyles, lesley.hoyles11@imperial.ac.uk; Simon McArthur, s.mcarthur@qmul.ac.uk

Running title: Propionate affects the blood–brain barrier

Abbreviations: ADHD, attention-deficit hyperactivity disorder; ASD, autism spectrum disorder; BBB, blood–brain barrier; CNS, central nervous system; FFAR, free fatty acid receptor; KEGG, Kyoto Encyclopaedia of Genes and Genomes; GO, Gene Ontology; LPS, lipopolysaccharide; SCFA, short-chain fatty acid; SPIA, Signalling Pathway Impact Analysis.

Abstract

Gut microbiome composition and function are symbiotically linked with host health, and altered in metabolic, inflammatory and neurodegenerative disorders. Three recognized mechanisms exist by which the microbiome influences the gut–brain axis: modification of autonomic/sensorimotor connections, immune activation, and neuroendocrine pathway regulation. We hypothesized interactions between circulating gut-derived microbial metabolites and the blood–brain barrier (BBB) also contribute to the gut–brain axis. Propionate, produced from dietary substrates by colonic bacteria, stimulates intestinal gluconeogenesis and is associated with reduced stress behaviours, but its potential endocrine role has not been addressed. After demonstrating expression of the propionate receptor FFAR3 on human brain endothelium, we examined the impact of a physiologically relevant propionate concentration (1 μM) on BBB properties *in vitro*. Propionate inhibited pathways associated with non-specific microbial infections via a CD14-dependent mechanism, suppressed expression of LRP-1 and protected the BBB from oxidative stress via NRF2 (NFE2L2) signaling. Together, these results suggest gut-derived microbial metabolites interact with the BBB, representing a fourth facet of the gut–brain axis that warrants further attention.

Introduction

The human body plays host to, and exists in symbiosis with, a significant number of microbial communities, including those of the skin, oral and vaginal mucosae and, most prominently, the gut (Nicholson *et al*, 2012). This relationship extends beyond simple commensalism to represent a major regulatory influence in health and disease, with changes in abundance of members of the faecal microbiota having been associated with numerous pathologies, including diabetes, hepatic diseases, inflammatory bowel disease, viral infections and neurodegenerative disorders (Forslund *et al*, 2015; Ley *et al*, 2005; Manichanh *et al*, 2006; Turnbaugh *et al*, 2009; Qin *et al*, 2014; Monaco *et al*, 2016; Smith *et al*, 2013). Metagenomic studies have revealed reductions in microbial gene richness and changes in functional capabilities of the faecal microbiome to be signatures of obesity, liver disease and type II diabetes, and that these can be modified by dietary interventions (Campbell *et al*, 2016; Shoaie *et al*, 2015). The gut microbiome harbours 150 times more genes than the human genome, significantly increasing the repertoire of functional genes available to the host and contributing to the harvesting of energy from food (Zhu *et al*, 2010).

The primary form of communication within the gut microbe–human super-system is metabolic, but our understanding of the details of the cross-signalling pathways involved is limited. It is clear, however, that gut-derived microbial metabolites and products such as lipopolysaccharide (LPS) can influence human health both in the intestine and systemically (Patterson *et al*, 2014; Li *et al*, 2008), with reported effects ranging from mediation of xenobiotic toxicity (Zheng *et al*, 2013), through modification of the risk of preterm birth (Kindinger *et al*, 2016) to induction of epigenetic programming in multiple host tissues (Bhat & Kapila, 2017; Krautkramer *et al*, 2017). A major aspect of microbe–host systems level communication that is receiving increased attention is the influence the gut microbiota exerts upon the central nervous system (CNS), the so-called ‘gut–brain axis’ (Sherwin *et al*, 2016).

The existence of gut–brain communication is supported by a number of animal and human studies, although the underlying mechanisms are not always well defined. Behavioural analysis of antibiotic-treated or germ-free rodents reveals alterations in

both stress responsiveness (Sudo *et al*, 2004) and anxiety (Neufeld *et al*, 2011; Heijtz *et al*, 2011; Bercik *et al*, 2011), although in germ-free models these findings are complicated by the life-long absence of gut microbes and possible consequent developmental alterations. Nonetheless, gut-microbe-depleted animals have been shown to exhibit changes in serotonergic and glutamatergic neuronal signalling (Neufeld *et al*, 2011) and expression of brain-derived neurotrophic factor (BDNF) within the limbic system (Bercik *et al*, 2011; Hoban *et al*, 2016), providing a molecular correlate for behavioural changes.

Links between the gut microbiota and brain function have been identified in studies of humans with autism spectrum disorders (ASD) and attention-deficit hyperactivity disorder (ADHD). Altered microbial profiles have been identified in children with ASD (Finegold *et al*, 2012, 2010; Mezzelani *et al*, 2015), and oral treatment of autistic children with the non-absorbed, broad-spectrum antibiotic vancomycin – effectively suppressing the gut microbiota – led to a regression in autistic behavioural characteristics that was reversed upon antibiotic discontinuation (Sandler *et al*, 2000). Similarly, a small-scale intervention study has suggested not only a link between lower counts of faecal *Bifidobacterium* species at six months and increased incidence of ADHD at 13 years, but also that early probiotic treatment lessens the risk of ADHD development (Pärtty *et al*, 2015).

A number of unresolved questions remain as to the mechanism(s) of communication between the gut microbiota and the brain, but three major pathways have been proposed: direct modification of vagal or sympathetic sensorimotor function (Forsythe *et al*, 2014), inflammatory/immune activity (Powell *et al*, 2017) and neuroendocrine crosstalk (Cani & Knauf, 2016). Whilst research in this field has focussed most heavily on direct neural modulation and inflammatory signalling, the potential role of circulating gut microbe-derived metabolites has been relatively underexplored. Communication with and across the blood–brain barrier (BBB), the primary interface between the circulation and the CNS, may therefore represent a significant mechanism allowing the gut microbiota to influence brain function.

There is accumulating evidence that the gut microbiota can affect the integrity of the BBB, with both broad-spectrum-antibiotic-treated and germ-free mice exhibiting

considerably enhanced barrier permeability and dysregulation of inter-endothelial cell tight junctions (Braniste *et al*, 2014; Fröhlich *et al*, 2016). Importantly, these impairments can be reversed upon conventionalisation. The mechanism(s) by which gut microbes exert their influence are unclear, but changes to brain chemistry induced by alteration of the gut microbiota can occur independently of vagal or sympathetic neural pathways and in the absence of any immune response, strongly suggesting at least a contributory role for soluble gut-derived microbial metabolites (Bercik *et al*, 2011).

In particular, data highlight a potential role for short-chain fatty acids (SCFAs) as key microbial mediators in the gut–brain axis. SCFAs are principally produced by the fermentation of complex plant-based polysaccharides by gut bacteria and are potent bioactive molecules; stimulating colonic blood flow and upper-gut motility, influencing H_2O and NaCl uptake, providing energy for colonocytes, enhancing satiety and positively influencing metabolic health in obese and diabetic individuals (Roediger, 1980; Salminen *et al*, 1998; Frost *et al*, 2014). Of the SCFAs, acetate is produced in the greatest quantity as a result of fermentation in the large intestine, followed by propionate and butyrate (Cummings *et al*, 1987). Over 95 % of SCFAs produced are absorbed within the colon with virtually none appearing in the urine or faeces (Salminen *et al*, 1998; Topping & Clifton, 2001). However, all three metabolites are detectable in the peripheral blood of healthy individuals (http://www.hmdb.ca: acetate, 22–42 μM; propionate, 0.9–1.2 μM; butyrate, 0.3–1.5 μM). SCFAs activate members of the free fatty acid receptor (FFAR) family of G protein coupled receptors; acetate, propionate and butyrate have affinity in the low millimolar to high micromolar range for FFAR2; propionate and butyrate have mid to low micromolar affinity for FFAR3 (Alexander *et al*, 2015).

The majority of studies looking at the role of SCFAs in the gut–brain axis have focused on butyrate (Stilling *et al*, 2016), with relatively few investigating propionate despite its similar plasma concentration and receptor affinity. Propionate is a highly potent FFAR3 agonist (agonist activity GTPγS pEC_{50} (E_{max}) 3.99(100%))) and has close to optimal ligand efficiency ($-\Delta G$=1.26 kcal mol^{-1} $atom^{-1}$) for this receptor (Schmidt *et al*, 2011). Whilst propionate has been shown to stimulate intestinal gluconeogenesis through

direct stimulation of enteric–CNS pathways (De Vadder *et al*, 2014), and increased intestinal propionate has been associated with reduced stress behaviours (Burokas *et al*, 2017) and reward pathway activity (Byrne *et al*, 2016) in mice and humans, respectively, its potential role as an endocrine mediator in the gut–brain axis has not been addressed. Given the presence of FFAR3 on endothelial cells (Brown *et al*, 2003), we hypothesised that propionate targeting of the endothelium of the BBB would represent an additional facet of the gut–brain axis. We used a systems approach to test this proposal, performing an unbiased study of the transcriptomic effects of exposure to physiological levels of propionate upon the BBB, modelled by the immortalised human cerebromicrovascular endothelial cell line hCMEC/D3, accompanied by *in vitro* validation of identified pathway responses.

Results

Microarray analyses

Following initial confirmation of the expression of FFAR3 in human brain endothelium (**Fig. 1a**) and on hCMEC/D3 cells (**Fig. 1b**), we investigated the effect of exposure of hCMEC/D3 monolayers to 1 μM propionate for 24 h. Such treatment had a significant ($P_{FDR} < 0.1$) effect on the expression of 1136 genes: 553 upregulated, 583 downregulated (**Fig. 1c**). Initially, we used SPIA with all the significantly differentially expressed genes to identify KEGG signalling pathways inhibited and activated in the presence of propionate. Protein processing in the endoplasmic reticulum and RNA transport were activated upon exposure of cells to propionate, which was unsurprising given gene expression had been induced. A number of pathways associated with non-specific microbial infections (Gram-negative bacteria, viral) were inhibited by propionate (**Fig. 1d**), as were the cytosolic DNA-sensing pathway (upregulated by pathogen DNA during microbial infections, triggering innate immune signalling (Radoshevich & Dussurget, 2016)), the NFκB signalling pathway and the Toll-like receptor signalling pathway.

Enrichr (Chen *et al*, 2013; Kuleshov *et al*, 2016) was used to examine KEGG pathways significantly associated with the list of significantly differentially expressed genes. All 1136 significantly differentially expressed genes mapped to Enrichr. As with SPIA, the genes were associated with KEGG pathways implicated in non-specific microbial infections, and RNA- and endoplasmic reticulum-associated processes (**Fig. 1e**).

WikiPathways analysis (Enrichr) of all the significantly differentially expressed genes highlighted responses to oxidative stress being associated with propionate treatment (not shown). Closer examination of the data demonstrated this was linked to NRF2 (NFE2L2) signaling, with the significantly upregulated genes closely associated with oxidative stress responses (**Fig. 1f**).

Pathway validation

Transcriptomic analysis identified two particular clusters of pathways as being regulated by propionate treatment: those involved in the non-specific inflammatory response to microbial products (**Fig. 1d, e**) and those involved in the response to

oxidative stress (**Fig. 1f**). We, therefore, sought to validate these responses in an *in vitro* model of the BBB.

TLR-specific pathway

Inhibition of the TLR-specific pathway by propionate suggests this metabolite may have a protective role against exposure of the BBB to bacterial lipopolysaccharide (LPS), derived from the cell walls of Gram-negative bacteria. In accord with this hypothesis, exposure of hCMEC/D3 monolayers for 12 h to propionate at physiological concentrations (1 μM) was able to significantly attenuate the permeabilising effects of exposure to *Escherichia coli* O111:B4 LPS (subsequent 12 h stimulation, 50 ng/ml), measured both through paracellular permeability to a 70 kDa FITC-conjugated dextran tracer (**Fig. 2a**) and trans-endothelial electrical resistance (**Fig. 2b**).

Paracellular permeability and trans-endothelial electrical resistance are in large part dependent upon the integrity of inter-endothelial tight junctions (Haseloff *et al*, 2015), which are known to be disrupted following exposure to LPS (Varatharaj & Galea, 2016). We, therefore, examined the intracellular distribution of the key tight junction components occludin, claudin-5 and zona occludens-1 (ZO-1) following treatment with propionate and/or LPS. Exposure of hCMEC/D3 monolayers to propionate alone (1 μM, 24 h) had no noticeable effect on the intracellular distribution of any of the studied tight junction components, whereas treatment with LPS (50 ng/ml, 12 h) caused a marked disruption in the localisation of all three major tight junction molecules, characterised by a loss of peri-membrane immunoreactivity (**Fig. 2c**). Notably, these effects of LPS were substantially protected against by prior treatment for 12h with 1 μM propionate.

LPS initiates a pro-inflammatory response through binding to Toll-like receptor 4, TLR4, in a complex with the accessory proteins CD14 and LY96 (MD2) (Peri *et al*, 2010); we, therefore, examined expression of TLR4 signalling components as an explanation for the protective effects of propionate upon this pathway. Whilst propionate treatment of hCMEC/D3 cells (1 μM, 24 h) had no significant effect upon expression of mRNA for TLR4 or LY96 (data not shown), such treatment significantly down-regulated expression of *CD14* mRNA (**Fig. 2d**), an effect replicated at the level of cell surface CD14 protein expression (**Fig. 2e, f**).

NFE2L2 (NRF2) signalling and protection from oxidative stress

Enrichr (WikiPathways) analysis indicated that exposure of hCMEC/D3 cells to propionate resulted in the regulation of a number of antioxidant systems. Searches of the genes associated with each of the individual pathways referenced in **Fig. 1f** strongly indicated these changes occurred downstream of the transcription factor nuclear factor, erythroid 2 like 2 – NFE2L2 (**Fig. 3a**). Supporting this analysis, exposure of hCMEC/D3 cells for 24 h to 1 μM propionate caused a marked translocation of NFE2L2 from the cytoplasm to the nucleus (**Fig. 3b**). Functional analysis of antioxidant pathway activity was assessed by monitoring reactive oxygen species production in hCMEC/D3 cells following exposure to the mitochondrial complex I inhibitor rotenone (2.5 μM, 2 h). Pre-exposure of cells to 1 μM propionate for 24 h significantly attenuated the rate of fluorescent tracer accumulation, indicative of reduced levels of intracellular reactive oxygen species (**Fig. 3c**).

Efflux transporter expression and activity

A key feature of the BBB is the expression of a wide array of efflux transporter proteins, acting to retard entry to and promote export from the brain for numerous endogenous and xenobiotic agents, amongst which the proteins P-glycoprotein, BCRP and LRP-1 are prominent examples. We investigated the ability of propionate to both modify expression of these transporters and, in the case of the ABC transporter proteins P-glycoprotein and BCRP, serve as a direct inhibitor or substrate for the protein. Exposure of hCMEC/D3 monolayers to propionate at physiological levels (1 μM) for 24 h significantly suppressed expression of LRP-1 without modulating expression of either BCRP or P-glycoprotein (**Expanded View Fig. 1a, b**). Similarly, propionate had neither a stimulatory nor inhibitory effect upon either BCRP or P-glycoprotein activity, at concentrations between 12 nM and 27 μM (**Expanded View Fig. 1c-f**).

Discussion

Considerable effort has gone into interrogating the gut–brain axis over recent years, with a steadily growing appreciation of the influence of the gut microbiota upon CNS function in health and disease. Mechanistic studies have identified three principal aspects to the gut–brain axis: modification of autonomic sensorimotor connections (Forsythe *et al*, 2014), immune activation (Powell *et al*, 2017), and regulation of neuroendocrine pathways (Cani & Knauf, 2016), all of which incorporate a role for soluble gut-derived microbial agents, whether metabolic products or structural microbial components (e.g. LPS) themselves. In the current study, we identify a fourth facet to the gut–brain axis, namely the interactions between gut-derived microbial metabolites and the primary defensive structure of the brain, the BBB. In particular, we identify a beneficial, protective effect of the SCFA propionate upon the BBB, mitigating against deleterious inflammatory and oxidative stimuli.

These protective effects of propionate upon BBB endothelial cells add to the previously described beneficial actions of the SCFA upon a number of metabolic parameters. Propionate has been shown to improve glucose tolerance and insulin sensitivity, reduce high-density lipoprotein and increase serum triglyceride concentrations (Salminen *et al*, 1998; Todesco *et al*, 1991; Venter *et al*, 1990), all of which result in a more stable metabolic homeostasis. The effects of propionate upon the BBB that we describe in this study add to these pro-homeostatic actions, emphasising the contribution the SCFA plays to maintaining normal physiological function. Given that the main source of circulating propionate in humans is the colonic microbiota (Reichardt *et al*, 2014; Vogt & Wolever, 2003), following fermentation of non-digestible carbohydrates by select bacterial species (**Fig. 4**), propionate thus represents a paradigm of commensal, mutually beneficial interactions between the host and microbiota. In particular, as consumption of food containing non-digestible carbohydrates increases circulating propionate concentrations (Vogt *et al*, 2004) the anti-inflammatory effects of the SCFA upon the cerebrovascular endothelium may be another facet of the known health benefits of high-fibre diets (Russell *et al*, 2013).

That BBB integrity is influenced by the gut microbiota and that SCFAs may play a role in this process was recently emphasised in studies of germ-free *vs.* specific pathogen-free mice, with germ-free animals exhibiting enhanced BBB permeability and disrupted cerebral endothelial tight junctions (Braniste *et al*, 2014). These permeability defects were reversed fully upon conventionalisation with a pathogen-free microbiota, and partially with monocultures producing various SCFAs. Moreover, defective BBB integrity could be ameliorated at least partially by extended oral administration of sodium butyrate. Our findings thus cement SCFAs as a key group of gut-derived microbial mediators modulating BBB function, and provide evidence emphasising a direct action through the circulation. Propionate acts primarily through either of the two free fatty acid receptors FFAR2 or FFAR3 (Schmidt *et al*, 2011), which although absent from neurones in the CNS (Nohr *et al*, 2015) have been identified in the cerebral endothelium (Brown *et al*, 2003), confirmed herein, indicating a possible mechanism of action. The relative importance of different SCFAs in regulating BBB function requires further study, given variation in both SCFA abundance and potency at FFAR2/FFAR3, and differences in signalling systems triggered by these receptors, but redundancy in SCFA effects upon the BBB may be indicative of their significance in normal physiology.

Notably, and perhaps unsurprisingly, SCFAs cannot fully recapitulate the BBB-restoring effects of conventionalisation of germ-free animals, as revealed in the current work and previously (Braniste *et al*, 2014; Fröhlich *et al*, 2016). It, therefore, seems likely that additional circulating gut-derived microbial mediators may contribute to the regulation of BBB function, and are thus highly deserving of future investigation. Given that upwards of 200 distinct microbial metabolites have been identified in the circulation of healthy individuals and animals (Zheng *et al*, 2011; Russell *et al*, 2013), there is clearly great potential for intestinal dysbiosis and the resultant variation in metabolite levels to impact upon the BBB.

This may be highly relevant to the development of neurological disease, as variation in BBB function is increasingly recognised to impact on cognitive processes, although the mechanism(s) underlying this link are poorly understood. In particular, defects in BBB integrity have been linked with impaired memory (Montagne *et al*, 2015) and

linguistic (Taheri *et al*, 2011) function, as well as with inferior performance on psychometric tests such as the mini mental state exam (Bowman *et al*, 2007) and Oxford handicap scale (Wardlaw *et al*, 2013). Antibiotic-induced intestinal dysbiosis has been associated with similar cognitive deficits and with a reduction in circulating gut-derived microbial metabolites (Fröhlich *et al*, 2016), but as yet whether the BBB plays a role in this connection has not been investigated. If this is the case, however, as the current study suggests, regulation of BBB function by microbe-derived mediators may be an important component in some of the emerging links between intestinal dysbiosis and pathologies as significant as depression (Aizawa *et al*, 2016), Parkinson's disease (Scheperjans *et al*, 2015; Petrov *et al*, 2017) and Alzheimer's disease (Cattaneo *et al*, 2017). Notably, patients with early Parkinson's or Alzheimer's diseases have been shown to bear reduced levels of *Bacteroides* species within the colon (Bedarf *et al*, 2017; Cattaneo *et al*, 2017). Given that *Bacteroides* spp. are important producers of SCFAs, including propionate (Reichardt *et al*, 2014), from complex carbohydrates (**Fig. 4**), this reduction may lead to a decline in circulating propionate and consequent vulnerability of the BBB, and, by extension, the brain in these major neurological conditions.

Modulatory effects of circulating gut-derived microbial metabolites upon the BBB may also be a component of the beneficial outcomes seen upon consumption of prebiotics or probiotics in a number of neurological conditions. For example, small-scale clinical trials have identified beneficial effects of probiotic drinks on cognitive ability in both Alzheimer's disease (Akbari *et al*, 2016) and multiple sclerosis (Kouchaki *et al*, 2016), conditions associated with reduced BBB integrity (Engelhardt & Sorokin, 2009). Similarly, oral administration of prebiotic oligosaccharides to mice significantly reduced anxiety and stress behaviours, effects that correlated with increases in caecal acetate, propionate and butyrate concentrations (Burokas *et al*, 2017). Whether such changes in caecal SCFA reflected plasma levels was not measured, but given the ability of SCFAs to diffuse passively across the gut epithelium (Vogt & Wolever, 2003), increases in circulating concentrations may be likely. That inflammation contributes to depression has become clearer over recent years (Pariante, 2017), hence it is conceivable that the anti-inflammatory effects of propionate we describe may underlie at least part of the

protective effects of prebiotic treatment, a proposal which, though speculative, is deserving of further study.

In summary, we reveal here a significant new aspect of the gut–brain axis, namely the modulatory effects of circulating gut-derived microbial metabolites upon the endothelium of the BBB. Given the critical gate-keeping role the BBB plays in communication between the periphery and the brain parenchyma, our findings set the stage for future investigation of the influence the gut microbiota has on this structure, and the impact intestinal dysbiosis may have upon individual susceptibility to neurological and psychological diseases.

Materials & Methods

Human Tissue

Human post mortem samples were taken from the prefrontal cortex from non-neurologic controls; brains were retrieved from the UK Multiple Sclerosis Society tissue bank at Imperial College London, under ethical approval from the UK MRC Brain Bank Network (Ref. No. 08/MRE09/31+5). Brains were selected according to the following criteria: (i) availability of full clinical history, (ii) no evidence of cancer post mortem, and (iii) negligible atherosclerosis of cerebral vasculature. Tissue was fixed in 10% v/v buffered formalin and embedded in paraffin. From each paraffin block, 5 µm sections were cut and used for immunohistochemistry for FFAR3 using standard protocols (Cristante *et al*, 2013), with a primary rabbit anti-FFAR3 polyclonal antibody (1:100; Stratech Scientific, Newmarket, UK), a horseradish peroxidase-conjugated goat anti-rabbit secondary antibody (1:300; Stratech Scientific, UK), and 2,3-diaminobenzidine and hydrogen peroxide as chromogens. Images were taken using a Leica DM5000 bright-field microscope equipped with a x40 oil immersion objective, and analysed using NIH ImageJ 1.51h (National Institutes of Health, USA).

hCMEC/D3 cell line

The human cerebromicrovascular endothelial cell line hCMEC/D3 was maintained and treated as described previously (Weksler *et al*, 2005; Cristante *et al*, 2013; Maggioli *et al*, 2015). Cells were cultured to confluency in complete EGM-2 endothelial cell growth medium (Lonza, Basel, Switzerland), whereupon medium was replaced by EGM-2 without VEGF and cells were further cultured for a minimum of 4 days to enable intercellular tight junction formation prior to experimentation.

Microarrays

hCMEC/D3 cells were grown on 6-well plates coated with calf-skin collagen (Sigma-Aldrich, Gillingham, UK) to confluency as described above, further cultured for 4 days in EGM-2 medium without VEGF and exposed to propionate (1 µM, 24 h). Cells were collected into TRIzol (Thermo-Fisher Scientific, UK) and total RNA was extracted using a TRIzol Plus RNA purification kit (Thermo-Fisher Scientific, UK) and quantified using an ND-1000 Spectrophotometer (NanoDrop, Wilmington, USA).

Hybridization experiments were performed by Macrogen Inc. (Seoul, Korea) using Illumina HumanHT-12 v4.0 Expression BeadChips (Illumina Inc., San Diego, CA). RNA purity and integrity were evaluated using an ND-1000 Spectrophotometer (NanoDrop, USA) and an Agilent 2100 Bioanalyzer (Agilent Technologies, Palo Alto, USA). Total RNA was amplified and purified using TargetAmp-Nano Labelling Kit for Illumina Expression BeadChip (EPICENTRE, Madison, USA) to yield biotinylated cRNA according to the manufacturer's instructions. Briefly, 350 ng of total RNA was reverse-transcribed to cDNA using a T7 oligo(dT) primer. Second-strand cDNA was synthesized, *in vitro*-transcribed, and labelled with biotin-NTP. After purification, the cDNA was quantified using the ND-1000 Spectrophotometer (NanoDrop, USA).

Labelled (750 ng) cDNA samples were hybridized to each beadchip for 17 h at 58 °C, according to the manufacturer's instructions. Detection of array signal was carried out using Amersham fluorolink streptavidin-Cy3 (GE Healthcare Bio-Sciences, Little Chalfont, UK) following the bead array manual. Arrays were scanned with an Illumina bead array reader confocal scanner according to the manufacturer's instructions. The quality of hybridization and overall chip performance were monitored by visual inspection of both internal quality control checks and the raw scanned data. Raw data were extracted using the software provided by the manufacturer (Illumina GenomeStudio v2011.1, Gene Expression Module v1.9.0).

Processing and analyses of array data

Raw data supplied by Macrogen were quality-checked, $\log_2$-transformed and loess-normalized (2 iterations) using affy (Gautier *et al*, 2004). Probes annotated as 'Bad' or 'No match' in illuminaHumanv4.db (Dunning *et al*, 2015) were removed from the dataset (n = 13,631) (Ritchie *et al*, 2011). After this filtering step, only probes with valid Entrez identifiers (n = 28,979) were retained for further analyses. Entrez identifiers were matched to official gene symbols using 'Homo_sapiens.gene_info', downloaded from https://www.ncbi.nlm.nih.gov/guide/genes-expression/ on 14 January 2017. Average gene expression values were used for identification of differentially expressed genes. Array data have been deposited in ArrayExpress under accession number E-MTAB-5686.

Signaling Pathway Impact Analysis (SPIA) was used to identify Kyoto Encyclopedia of Genes and Genomes (KEGG) pathways activated or inhibited in hCMEC/D3 cells exposed to propionate (Tarca *et al*, 2009). Enrichr (Chen *et al*, 2013; Kuleshov *et al*, 2016) was used to confirm KEGG findings (with respect to pathways, not their activation/inhibition) and to perform Gene Ontology (GO)- and WikiPathways-based analyses.

In vitro barrier function assessments

Paracellular permeability and transendothelial electrical resistance were measured on 100 % confluent cultures polarised by growth on 24-well plate polyethylene terephthalate (PET) transwell inserts (surface area: 0.33 cm^2, pore size: 0.4 µm; Appleton Woods, UK) coated with calf-skin collagen and fibronectin (Sigma-Aldrich, UK). The permeability of hCMEC/D3 cell monolayers to 70 kDa FITC-dextran (2 mg/ml) was measured as described previously (Abbott *et al*, 1992; Coisne *et al*, 2005; Maggioli *et al*, 2015). Transendothelial electrical resistance (TEER) measurements were performed using a Millicell ERS-2 Voltohmmeter (Millipore, Watford, UK) and were expressed as $\Omega.cm^2$. In all cases, values obtained from cell-free inserts similarly coated with collagen and fibronectin were subtracted from the total values. Briefly, cells were treated with propionate (1 µM) for 24 hours prior to analysis of barrier function. In some cases, barrier integrity was tested by challenge with bacterial lipopolysaccharide (LPS). Confluent hCMEC/D3 monolayers were treated with propionate (1 µM) for 12 hours, whereupon LPS (*Escherichia coli* 0111:B4; 50 ng/ml, comparable to circulating levels of LPS in human endotoxemia (Pais de Barros *et al*, 2015)) was added for a further 12 hours, without wash-out. Barrier function characteristics were then interrogated as described above.

Efflux transporter assays

Activity of the major efflux transporters P-glycoprotein and BCRP (Löscher & Potschka, 2005) was determined through the use of commercially available assays (Solvo Biotechnology Inc., Budapest, Hungary), performed according to the manufacturer's instructions. Step-wise dose-response curves centred around reported physiological circulating concentrations of propionate (Wishart *et al*, 2013) were constructed (n=2) and both activating and inhibitory effects of propionate upon transporter activity were analysed.

Flow cytometry analysis

hCMEC/D3 cells were labelled with APC-conjugated mouse monoclonal anti-CD14 (Thermo-Fisher Scientific, Paisley, UK), APC-conjugated mouse monoclonal anti-BCRP (BD Biosciences, Oxford, UK), FITC-conjugated mouse monoclonal LRP1 (BD Biosciences, UK), PE-conjugated mouse monoclonal anti-MDR1A (BD Biosciences, UK), unconjugated rabbit polyclonal antibody directed against FFAR3/GPR41 (Flarebio Biotech LLC, College Park, MD, USA) followed by incubation with an AF488-conjugated goat anti-rabbit secondary antibody (Thermo-Fisher Scientific, UK), or appropriate isotype controls (all BD Biosciences, UK) for analysis by flow cytometry. Briefly, hCMEC/D3 cells were treated for 24 h with propionate (1 μM), detached using 0.05 % trypsin and incubated with antibodies as described above. Immunofluorescence was analysed for 20,000 events per treatment using a BD FACSCanto II (BD Biosciences, UK) flow cytometer and data were analysed using FlowJo 8.0 software (Treestar Inc., CA, USA).

Immunofluorescence analysis

hCMEC/D3 cells were cultured on Lab-Tek™ Permanox™ 8-well chamber slides coated with calf-skin collagen (Sigma-Aldrich, UK), prior to immunostaining according to standard protocols (Cristante *et al*, 2013; Maggioli *et al*, 2015) and using primary antibodies directed against Nrf2 (1:500, Novus Biologicals Ltd., Abingdon, UK), occludin (1:200, Thermo-Fisher Scientific, UK), claudin-5 (1:200, Thermo-Fisher Scientific, UK) and zona occludens-1 (ZO-1; 1:100, Thermo-Fisher Scientific, UK). Nuclei were counterstained with DAPI (Sigma-Aldrich, UK). Images were captured using an LSM880 confocal laser scanning microscope (Carl Zeiss Ltd., Cambridge, UK) fitted with 405 nm, 488 nm, and 561 nm lasers, and a 63x oil immersion objective lens (NA, 1.4 mm, working distance, 0.17 mm). Images were captured with ZEN imaging software (Carl Zeiss Ltd., UK) and analysed using ImageJ 1.51h (National Institutes of Health, USA).

Statistical analyses

Sample sizes were calculated to detect differences of 15 % or more with a power of 0.85 and α set at 5 %, calculations being informed by previously published data (Cristante *et al*, 2013; Maggioli *et al*, 2015). *In vitro* experimental data are expressed

as mean ± SEM, with *n*=3 independent experiments performed in triplicate for all studies. In all cases, normality of distribution was established using the Shapiro–Wilkes test, followed by analysis with two-tailed Student's *t*-tests to compare two groups or, for multiple comparison analysis, 1- or 2-way ANOVA followed by Tukey's HSD *post hoc* test. Where data was not normally distributed, non-parametric analysis was performed using the Wilcoxon signed rank test. A *P* value of less than or equal to 5 % was considered significant. Differentially expressed genes were identified in microarray data using LIMMA (Ritchie *et al*, 2015); *P* values were corrected for multiple testing using the Benjamini–Hochberg procedure (False Discovery Rate); a *P* value of less than or equal to 10 % was considered significant in this case.

Acknowledgements

This work was funded by Alzheimer's Research UK Pilot Grant no. ARUK-PPG2016B-6. This work used the computing resources of the UK MEDical BIOinformatics partnership – aggregation, integration, visualization and analysis of large, complex data (UK MED-BIO), which is supported by the Medical Research Council (grant number MR/L01632X/1). Human tissue samples and associated clinical and neuropathological data were supplied by the Multiple Sclerosis Society Tissue Bank, funded by the Multiple Sclerosis Society of Great Britain and Northern Ireland, registered charity 207495. LH is in receipt of an MRC Intermediate Research Fellowship in Data Science (MR/L01632X/1, UK MED-BIO). TS received a bursary from Imperial College London as part of the Undergraduate Research Opportunities Programme.

Author contributions

LH and SM conceived the experiments; LH, TS, UU and SM performed experiments; LH and SM analysed the data; LH and SM wrote the paper; JKN, SRC and RCG provided valuable insight and advice throughout the project.

Conflict of interest

The authors declare that they have no conflict of interest

References

Abbott NJ, Hughes CC, Revest PA & Greenwood J (1992) Development and characterisation of a rat brain capillary endothelial culture: towards an in vitro blood-brain barrier. *J. Cell Sci.* **103 (Pt 1:** 23–37

Aizawa E, Tsuji H, Asahara T, Takahashi T, Teraishi T, Yoshida S, Ota M, Koga N, Hattori K & Kunugi H (2016) Possible association of Bifidobacterium and Lactobacillus in the gut microbiota of patients with major depressive disorder. *J. Affect. Disord.* **202:** 254–257

Akbari E, Asemi Z, Daneshvar Kakhaki R, Bahmani F, Kouchaki E, Tamtaji OR, Hamidi GA & Salami M (2016) Effect of Probiotic Supplementation on Cognitive Function and Metabolic Status in Alzheimer's Disease: A Randomized, Double-Blind and Controlled Trial. *Front. Aging Neurosci.* **8:** 256

Alexander SP, Davenport AP, Kelly E, Marrion N, Peters JA, Benson HE, Faccenda E, Pawson AJ, Sharman JL, Southan C & Davies JA (2015) The Concise Guide to PHARMACOLOGY 2015/16: G protein-coupled receptors. *Br. J. Pharmacol.* **172:** 5744–5869

Bedarf JR, Hildebrand F, Coelho LP, Sunagawa S, Bahram M, Goeser F, Bork P & Wüllner U (2017) Functional implications of microbial and viral gut metagenome changes in early stage L-DOPA-naive Parkinson's disease patients. *Genome Med.* **9:** 39

Bercik P, Denou E, Collins J, Jackson W, Lu J, Jury J, Deng Y, Blennerhassett P, Macri J, McCoy KD, Verdu EF & Collins SM (2011) The intestinal microbiota affect central levels of brain-derived neurotropic factor and behavior in mice. *Gastroenterology* **141:** 599–609, 609–3

Bhat MI & Kapila R (2017) Dietary metabolites derived from gut microbiota: critical modulators of epigenetic changes in mammals. *Nutr. Rev.*

Bowman GL, Kaye JA, Moore M, Waichunas D, Carlson NE & Quinn JF (2007) Blood-brain barrier impairment in Alzheimer disease: stability and functional significance. *Neurology* **68:** 1809–14

Braniste V, Al-Asmakh M, Kowal C, Anuar F, Abbaspour A, Tóth M, Korecka A, Bakocevic N, Ng LG, Guan NL, Kundu P, Gulyás B, Halldin C, Hultenby K, Nilsson H, Hebert H, Volpe BT, Diamond B & Pettersson S (2014) The gut microbiota influences blood-brain barrier permeability in mice. *Sci. Transl. Med.* **6:** 263ra158

Brown AJ, Goldsworthy SM, Barnes AA, Eilert MM, Tcheang L, Daniels D, Muir AI, Wigglesworth MJ, Kinghorn I, Fraser NJ, Pike NB, Strum JC, Steplewski KM, Murdock PR, Holder JC, Marshall FH, Szekeres PG, Wilson S, Ignar DM, Foord SM, et al (2003) The Orphan G protein-coupled receptors GPR41 and GPR43 are activated by propionate and other short chain carboxylic acids. *J. Biol. Chem.* **278:** 11312–9

Burokas A, Arboleya S, Moloney RD, Peterson VL, Murphy K, Clarke G, Stanton C, Dinan TG & Cryan JF (2017) Targeting the Microbiota-Gut-Brain Axis: Prebiotics Have Anxiolytic and Antidepressant-like Effects and Reverse the Impact of Chronic Stress in Mice. *Biol. Psychiatry*

Byrne CS, Chambers ES, Alhabeeb H, Chhina N, Morrison DJ, Preston T, Tedford C, Fitzpatrick J, Irani C, Busza A, Garcia-Perez I, Fountana S, Holmes E, Goldstone AP & Frost GS (2016) Increased colonic propionate reduces anticipatory reward responses in the human striatum to high-energy foods. *Am. J. Clin. Nutr.* **104:** 5–14

Campbell SC, Wisniewski PJ, Noji M, McGuinness LR, Häggblom MM, Lightfoot SA,

Joseph LB & Kerkhof LJ (2016) The Effect of Diet and Exercise on Intestinal Integrity and Microbial Diversity in Mice. *PLoS One* **11:** e0150502

Cani PD & Knauf C (2016) How gut microbes talk to organs: The role of endocrine and nervous routes. *Mol. Metab.* **5:** 743–52

Cattaneo A, Cattane N, Galluzzi S, Provasi S, Lopizzo N, Festari C, Ferrari C, Guerra UP, Paghera B, Muscio C, Bianchetti A, Volta GD, Turla M, Cotelli MS, Gennuso M, Prelle A, Zanetti O, Lussignoli G, Mirabile D, Bellandi D, et al (2017) Association of brain amyloidosis with pro-inflammatory gut bacterial taxa and peripheral inflammation markers in cognitively impaired elderly. *Neurobiol. Aging* **49:** 60–68

Chen EY, Tan CM, Kou Y, Duan Q, Wang Z, Meirelles GV, Clark NR & Ma'ayan A (2013) Enrichr: interactive and collaborative HTML5 gene list enrichment analysis tool. *BMC Bioinformatics* **14:** 128

Coisne C, Dehouck L, Faveeuw C, Delplace Y, Miller F, Landry C, Morissette C, Fenart L, Cecchelli R, Tremblay P & Dehouck B (2005) Mouse syngenic in vitro blood-brain barrier model: a new tool to examine inflammatory events in cerebral endothelium. *Lab. Invest.* **85:** 734–46

Cristante E, McArthur S, Mauro C, Maggioli E, Romero IA, Wylezinska-Arridge M, Couraud PO, Lopez-Tremoleda J, Christian HC, Weksler BB, Malaspina A & Solito E (2013) Identification of an essential endogenous regulator of blood-brain barrier integrity, and its pathological and therapeutic implications. *Proc. Natl. Acad. Sci. U. S. A.* **110:** 832–841

Cummings JH, Pomare EW, Branch WJ, Naylor CP & Macfarlane GT (1987) Short chain fatty acids in human large intestine, portal, hepatic and venous blood. *Gut* **28:** 1221–7

Dunning M, Lynch A & Eldridge M (2015) illuminaHumanv4.db: Illumina HumanHT12v4 annotation data (chip illuminaHumanv4).

Elliott P, Posma JM, Chan Q, Garcia-Perez I, Wijeyesekera A, Bictash M, Ebbels TMD, Ueshima H, Zhao L, van Horn L, Daviglus M, Stamler J, Holmes E & Nicholson JK (2015) Urinary metabolic signatures of human adiposity. *Sci. Transl. Med.* **7:** 285ra62

Engelhardt B & Sorokin L (2009) The blood-brain and the blood-cerebrospinal fluid barriers: function and dysfunction. *Semin. Immunopathol.* **31:** 497–511

Finegold SM, Dowd SE, Gontcharova V, Liu C, Henley KE, Wolcott RD, Youn E, Summanen PH, Granpeesheh D, Dixon D, Liu M, Molitoris DR & Green JA (2010) Pyrosequencing study of fecal microflora of autistic and control children. *Anaerobe* **16:** 444–53

Finegold SM, Downes J & Summanen PH (2012) Microbiology of regressive autism. *Anaerobe* **18:** 260–2

Forslund K, Hildebrand F, Nielsen T, Falony G, Le Chatelier E, Sunagawa S, Prifti E, Vieira-Silva S, Gudmundsdottir V, Krogh Pedersen H, Arumugam M, Kristiansen K, Voigt AY, Vestergaard H, Hercog R, Igor Costea P, Kultima JR, Li J, Jørgensen T, Levenez F, et al (2015) Disentangling type 2 diabetes and metformin treatment signatures in the human gut microbiota. *Nature* **528:** 262–6

Forsythe P, Bienenstock J & Kunze WA (2014) Vagal pathways for microbiome-brain-gut axis communication. *Adv. Exp. Med. Biol.* **817:** 115–33

Fröhlich EE, Farzi A, Mayerhofer R, Reichmann F, Jačan A, Wagner B, Zinser E, Bordag N, Magnes C, Fröhlich E, Kashofer K, Gorkiewicz G & Holzer P (2016) Cognitive Impairment by Antibiotic-Induced Gut Dysbiosis: Analysis of Gut Microbiota-Brain Communication. *Brain. Behav. Immun.*

Frost G, Sleeth ML, Sahuri-Arisoylu M, Lizarbe B, Cerdan S, Brody L, Anastasovska J, Ghourab S, Hankir M, Zhang S, Carling D, Swann JR, Gibson G, Viardot A, Morrison D, Louise Thomas E & Bell JD (2014) The short-chain fatty acid acetate reduces appetite via a central homeostatic mechanism. *Nat. Commun.* **5:** 672–679

Gautier L, Cope L, Bolstad BM & Irizarry RA (2004) affy--analysis of Affymetrix GeneChip data at the probe level. *Bioinformatics* **20:** 307–15

Gorrini C, Harris IS & Mak TW (2013) Modulation of oxidative stress as an anticancer strategy. *Nat. Rev. Drug Discov.* **12:** 931–47

Haseloff RF, Dithmer S, Winkler L, Wolburg H & Blasig IE (2015) Transmembrane proteins of the tight junctions at the blood-brain barrier: structural and functional aspects. *Semin. Cell Dev. Biol.* **38:** 16–25

Heijtz RD, Wang S, Anuar F, Qian Y, Bjorkholm B, Samuelsson A, Hibberd ML, Forssberg H & Pettersson S (2011) Normal gut microbiota modulates brain development and behavior. *Proc. Natl. Acad. Sci.* **108:** 3047–3052

Hoban AE, Moloney RD, Golubeva AV, McVey Neufeld KA, O'Sullivan O, Patterson E, Stanton C, Dinan TG, Clarke G & Cryan JF (2016) Behavioural and neurochemical consequences of chronic gut microbiota depletion during adulthood in the rat. *Neuroscience* **339:** 463–477

Kindinger LM, MacIntyre DA, Lee YS, Marchesi JR, Smith A, McDonald JAK, Terzidou V, Cook JR, Lees C, Israfil-Bayli F, Faiza Y, Toozs-Hobson P, Slack M, Cacciatore S, Holmes E, Nicholson JK, Teoh TG & Bennett PR (2016) Relationship between vaginal microbial dysbiosis, inflammation, and pregnancy outcomes in cervical cerclage. *Sci. Transl. Med.* **8:** 350ra102

Kouchaki E, Tamtaji OR, Salami M, Bahmani F, Daneshvar Kakhaki R, Akbari E, Tajabadi-Ebrahimi M, Jafari P & Asemi Z (2016) Clinical and metabolic response to probiotic supplementation in patients with multiple sclerosis: A randomized, double-blind, placebo-controlled trial. *Clin. Nutr.*

Krautkramer KA, Rey FE & Denu JD (2017) Chemical signaling between gut microbiota and host chromatin: What is your gut really saying? *J. Biol. Chem.***:** jbc.R116.761577

Kuleshov M V, Jones MR, Rouillard AD, Fernandez NF, Duan Q, Wang Z, Koplev S, Jenkins SL, Jagodnik KM, Lachmann A, McDermott MG, Monteiro CD, Gundersen GW & Ma'ayan A (2016) Enrichr: a comprehensive gene set enrichment analysis web server 2016 update. *Nucleic Acids Res.* **44:** W90-7

Ley RE, Bäckhed F, Turnbaugh P, Lozupone CA, Knight RD & Gordon JI (2005) Obesity alters gut microbial ecology. *Proc. Natl. Acad. Sci. U. S. A.* **102:** 11070–5

Li M, Wang B, Zhang M, Rantalainen M, Wang S, Zhou H, Zhang Y, Shen J, Pang X, Wei H, Chen Y, Lu H, Zuo J, Su M, Qiu Y, Jia W, Xiao C, Smith LM, Yang S, Holmes E, et al (2008) Symbiotic gut microbes modulate human metabolic phenotypes. *Proc. Natl. Acad. Sci.* **105:** 2117–2122

Löscher W & Potschka H (2005) Blood-brain barrier active efflux transporters: ATP-binding cassette gene family. *NeuroRx* **2:** 86–98

Maggioli E, Mcarthur S, Mauro C, Kieswich J, Kusters DHMHM, Reutelingsperger CPMPM, Yaqoob M & Solito E (2015) Estrogen protects the blood-brain barrier from inflammation-induced disruption and increased lymphocyte trafficking. *BRAIN, Behav. Immun.* **51:** 212–222

Manichanh C, Rigottier-Gois L, Bonnaud E, Gloux K, Pelletier E, Frangeul L, Nalin R, Jarrin C, Chardon P, Marteau P, Roca J & Dore J (2006) Reduced diversity of

faecal microbiota in Crohn's disease revealed by a metagenomic approach. *Gut* **55:** 205–11

Mezzelani A, Landini M, Facchiano F, Raggi ME, Villa L, Molteni M, De Santis B, Brera C, Caroli AM, Milanesi L & Marabotti A (2015) Environment, dysbiosis, immunity and sex-specific susceptibility: A translational hypothesis for regressive autism pathogenesis. *Nutr. Neurosci.* **18:** 145–161

Monaco CL, Gootenberg DB, Zhao G, Handley SA, Ghebremichael MS, Lim ES, Lankowski A, Baldridge MT, Wilen CB, Flagg M, Norman JM, Keller BC, Luévano JM, Wang D, Boum Y, Martin JN, Hunt PW, Bangsberg DR, Siedner MJ, Kwon DS, et al (2016) Altered Virome and Bacterial Microbiome in Human Immunodeficiency Virus-Associated Acquired Immunodeficiency Syndrome. *Cell Host Microbe* **19:** 311–22

Montagne A, Barnes SR, Sweeney MD, Halliday MR, Sagare AP, Zhao Z, Toga AW, Jacobs RE, Liu CY, Amezcua L, Harrington MG, Chui HC, Law M & Zlokovic BV (2015) Blood-Brain Barrier Breakdown in the Aging Human Hippocampus. *Neuron* **85:** 296–302

Neufeld KM, Kang N, Bienenstock J & Foster JA (2011) Reduced anxiety-like behavior and central neurochemical change in germ-free mice. *Neurogastroenterol. Motil.* **23:** 255-e119

Nicholson JK, Holmes E, Kinross J, Burcelin R, Gibson G, Jia W & Pettersson S (2012) Host-gut microbiota metabolic interactions. *Science* **336:** 1262–7

Nohr MK, Egerod KL, Christiansen SH, Gille A, Offermanns S, Schwartz TW & M?ller M (2015) Expression of the short chain fatty acid receptor GPR41/FFAR3 in autonomic and somatic sensory ganglia. *Neuroscience* **290:** 126–137

Pais de Barros J-P, Gautier T, Sali W, Adrie C, Choubley H, Charron E, Lalande C, Le Guern N, Deckert V, Monchi M, Quenot J-P & Lagrost L (2015) Quantitative lipopolysaccharide analysis using HPLC/MS/MS and its combination with the limulus amebocyte lysate assay. *J. Lipid Res.* **56:** 1363–9

Pariante CM (2017) Why are depressed patients inflamed? A reflection on 20 years of research on depression, glucocorticoid resistance and inflammation. *Eur. Neuropsychopharmacol.* **27:** 554–559

Pärtty A, Kalliomäki M, Wacklin P, Salminen S & Isolauri E (2015) A possible link between early probiotic intervention and the risk of neuropsychiatric disorders later in childhood: a randomized trial. *Pediatr. Res.* **77:** 823–828

Patterson E, Cryan JF, Fitzgerald GF, Ross RP, Dinan TG & Stanton C (2014) Gut microbiota, the pharmabiotics they produce and host health. *Proc. Nutr. Soc.* **73:** 477–489

Peri F, Piazza M, Calabrese V, Damore G & Cighetti R (2010) Exploring the LPS/TLR4 signal pathway with small molecules. *Biochem. Soc. Trans.* **38:** 1390–5

Petrov VA, Saltykova I V, Zhukova IA, Alifirova VM, Zhukova NG, Dorofeeva YB, Tyakht A V, Kovarsky BA, Alekseev DG, Kostryukova ES, Mironova YS, Izhboldina OP, Nikitina MA, Perevozchikova T V, Fait EA, Babenko V V, Vakhitova MT, Govorun VM & Sazonov AE (2017) Analysis of Gut Microbiota in Patients with Parkinson's Disease. *Bull. Exp. Biol. Med.* **162:** 734–737

Powell N, Walker MM & Talley NJ (2017) The mucosal immune system: master regulator of bidirectional gut–brain communications. *Nat. Rev. Gastroenterol. Hepatol.* **14:** 143–159

Qin N, Yang F, Li A, Prifti E, Chen Y, Shao L, Guo J, Le Chatelier E, Yao J, Wu L, Zhou J, Ni S, Liu L, Pons N, Batto JM, Kennedy SP, Leonard P, Yuan C, Ding W, Chen Y, et al (2014) Alterations of the human gut microbiome in liver cirrhosis.

Nature **513:** 59–64
Radoshevich L & Dussurget O (2016) Cytosolic Innate Immune Sensing and Signaling upon Infection. *Front. Microbiol.* **7:** 313
Reichardt N, Duncan SH, Young P, Belenguer A, McWilliam Leitch C, Scott KP, Flint HJ & Louis P (2014) Phylogenetic distribution of three pathways for propionate production within the human gut microbiota. *ISME J.* **8:** 1323–35
Ritchie ME, Dunning MJ, Smith ML, Shi W & Lynch AG (2011) BeadArray expression analysis using bioconductor. *PLoS Comput. Biol.* **7:** e1002276
Ritchie ME, Phipson B, Wu D, Hu Y, Law CW, Shi W & Smyth GK (2015) limma powers differential expression analyses for RNA-sequencing and microarray studies. *Nucleic Acids Res.* **43:** e47
Roediger WE (1980) Role of anaerobic bacteria in the metabolic welfare of the colonic mucosa in man. *Gut* **21:** 793–8
Russell WR, Hoyles L, Flint HJ & Dumas M-E (2013) Colonic bacterial metabolites and human health. *Curr. Opin. Microbiol.* **16:** 246–254
Salminen S, Bouley C, Boutron-Ruault MC, Cummings JH, Franck A, Gibson GR, Isolauri E, Moreau MC, Roberfroid M & Rowland I (1998) Functional food science and gastrointestinal physiology and function. *Br. J. Nutr.* **80 Suppl 1:** S147-71
Sandler RH, Finegold SM, Bolte ER, Buchanan CP, Maxwell AP, Vaisanen M-L, Nelson MN & Wexler HM (2000) Short-Term Benefit From Oral Vancomycin Treatment of Regressive-Onset Autism. *J. Child Neurol.* **15:** 429–435
Scheperjans F, Aho V, Pereira PAB, Koskinen K, Paulin L, Pekkonen E, Haapaniemi E, Kaakkola S, Eerola-Rautio J, Pohja M, Kinnunen E, Murros K & Auvinen P (2015) Gut microbiota are related to Parkinson's disease and clinical phenotype. *Mov. Disord.* **30:** 350–8
Schmidt J, Smith NJ, Christiansen E, Tikhonova IG, Grundmann M, Hudson BD, Ward RJ, Drewke C, Milligan G, Kostenis E & Ulven T (2011) Selective orthosteric free fatty acid receptor 2 (FFA2) agonists: identification of the structural and chemical requirements for selective activation of FFA2 versus FFA3. *J. Biol. Chem.* **286:** 10628–40
Sherwin E, Rea K, Dinan TG & Cryan JF (2016) A gut (microbiome) feeling about the brain. *Curr. Opin. Gastroenterol.* **32:** 96–102
Shoaie S, Ghaffari P, Kovatcheva-Datchary P, Mardinoglu A, Sen P, Pujos-Guillot E, de Wouters T, Juste C, Rizkalla S, Chilloux J, Hoyles L, Nicholson JK, Dore J, Dumas ME, Clement K, Bäckhed F, Nielsen J & Nielsen J (2015) Quantifying Diet-Induced Metabolic Changes of the Human Gut Microbiome. *Cell Metab.* **22:** 320–331
Smith MI, Yatsunenko T, Manary MJ, Trehan I, Mkakosya R, Cheng J, Kau AL, Rich SS, Concannon P, Mychaleckyj JC, Liu J, Houpt E, Li J V, Holmes E, Nicholson J, Knights D, Ursell LK, Knight R & Gordon JI (2013) Gut microbiomes of Malawian twin pairs discordant for kwashiorkor. *Science* **339:** 548–54
Stilling RM, van de Wouw M, Clarke G, Stanton C, Dinan TG & Cryan JF (2016) The neuropharmacology of butyrate: The bread and butter of the microbiota-gut-brain axis? *Neurochem. Int.* **99:** 110–132
Sudo N, Chida Y, Aiba Y, Sonoda J, Oyama N, Yu X-N, Kubo C & Koga Y (2004) Postnatal microbial colonization programs the hypothalamic-pituitary-adrenal system for stress response in mice. *J. Physiol.* **558:** 263–75
Taheri S, Gasparovic C, Huisa BN, Adair JC, Edmonds E, Prestopnik J, Grossetete M, Shah NJ, Wills J, Qualls C & Rosenberg GA (2011) Blood-brain barrier permeability abnormalities in vascular cognitive impairment. *Stroke.* **42:** 2158–63

Tarca AL, Draghici S, Khatri P, Hassan SS, Mittal P, Kim J-S, Kim CJ, Kusanovic JP & Romero R (2009) A novel signaling pathway impact analysis. *Bioinformatics* **25:** 75–82

Todesco T, Rao A V, Bosello O & Jenkins DJ (1991) Propionate lowers blood glucose and alters lipid metabolism in healthy subjects. *Am. J. Clin. Nutr.* **54:** 860–5

Topping DL & Clifton PM (2001) Short-chain fatty acids and human colonic function: roles of resistant starch and nonstarch polysaccharides. *Physiol. Rev.* **81:** 1031–64

Turnbaugh PJ, Hamady M, Yatsunenko T, Cantarel BL, Duncan A, Ley RE, Sogin ML, Jones WJ, Roe BA, Affourtit JP, Egholm M, Henrissat B, Heath AC, Knight R & Gordon JI (2009) A core gut microbiome in obese and lean twins. *Nature* **457:** 480–4

De Vadder F, Kovatcheva-Datchary P, Goncalves D, Vinera J, Zitoun C, Duchampt A, Bäckhed F & Mithieux G (2014) Microbiota-generated metabolites promote metabolic benefits via gut-brain neural circuits. *Cell* **156:** 84–96

Varatharaj A & Galea I (2016) The blood-brain barrier in systemic inflammation. *Brain. Behav. Immun.*

Venter CS, Vorster HH & Cummings JH (1990) Effects of dietary propionate on carbohydrate and lipid metabolism in healthy volunteers. *Am. J. Gastroenterol.* **85:** 549–53

Vogt JA, Pencharz PB & Wolever TMS (2004) L-Rhamnose increases serum propionate in humans. *Am. J. Clin. Nutr.* **80:** 89–94

Vogt JA & Wolever TMS (2003) Fecal acetate is inversely related to acetate absorption from the human rectum and distal colon. *J. Nutr.* **133:** 3145–8

Wardlaw JM, Doubal FN, Valdes-Hernandez M, Wang X, Chappell FM, Shuler K, Armitage PA, Carpenter TC & Dennis MS (2013) Blood-brain barrier permeability and long-term clinical and imaging outcomes in cerebral small vessel disease. *Stroke.* **44:** 525–7

Weksler BB, Subileau EA, Perrière N, Charneau P, Holloway K, Leveque M, Tricoire-Leignel H, Nicotra A, Bourdoulous S, Turowski P, Male DK, Roux F, Greenwood J, Romero IA & Couraud PO (2005) Blood-brain barrier-specific properties of a human adult brain endothelial cell line. *FASEB J.* **19:** 1872–4

Wishart DS, Jewison T, Guo AC, Wilson M, Knox C, Liu Y, Djoumbou Y, Mandal R, Aziat F, Dong E, Bouatra S, Sinelnikov I, Arndt D, Xia J, Liu P, Yallou F, Bjorndahl T, Perez-Pineiro R, Eisner R, Allen F, et al (2013) HMDB 3.0--The Human Metabolome Database in 2013. *Nucleic Acids Res.* **41:** D801–D807

Zheng X, Xie G, Zhao A, Zhao L, Yao C, Chiu NHL, Zhou Z, Bao Y, Jia W, Nicholson JK & Jia W (2011) The footprints of gut microbial-mammalian co-metabolism. *J. Proteome Res.* **10:** 5512–22

Zheng X, Zhao A, Xie G, Chi Y, Zhao L, Li H, Wang C, Bao Y, Jia W, Luther M, Su M, Nicholson JK & Jia W (2013) Melamine-induced renal toxicity is mediated by the gut microbiota. *Sci. Transl. Med.* **5:** 172ra22

Zhu B, Wang X & Li L (2010) Human gut microbiome: the second genome of human body. *Protein Cell* **1:** 718–725

Figure Legends

Fig. 1: Effects on gene expression of exposure of the hCMEC/D3 cell line to propionate (1 μM, 24 h). (a) Representative images of FFAR3 immunoreactivity within endothelial cells of capillaries (i) and larger post-capillary (ii) blood vessels in control human brains *post mortem*; scale bar 20 μm, sections are 5 μm thick; images are representative of five independent cases, areas of particular immunoreactivity are highlighted by black arrowheads (b) Surface expression of FFAR3/GPR41 by hCMEC/D3 cells (grey line, unstained cells, black line secondary antibody control, red line FFAR3), data are representative of three independent experiments. (c) Volcano plot showing significantly ($P_{FDR} < 0.1$, red dots) differentially expressed genes. The top 20 up- and down-regulated genes are labelled. (d) SPIA evidence plot for the 1136 significantly differentially expressed genes. Only those human KEGG pathways associated with non-specific microbial infections are labelled. The pathways at the right of the red oblique line are significant ($P < 0.2$) after Bonferroni correction of the global P values, pG, obtained by combining the pPERT and pNDE using the normal inversion method. The pathways at the right of the blue oblique line are significant ($P < 0.2$) after a FDR correction of the global P values, pG. 04810, Regulation of actin cytoskeleton (inhibited); 04064, NF-kappa B signaling pathway (inhibited); 04978, Mineral absorption (inhibited); 03013, RNA transport (activated); 04141, Protein processing in endoplasmic reticulum (activated); 04350, TGF-beta signaling pathway (activated); 04623, Cytosolic DNA-sensing pathway (inhibited). (e) Association of all significantly differentially expressed genes (n = 1136) with KEGG pathways, Enrichr. (f) Association of all significantly upregulated genes (n = 553) with WikiPathways, Enrichr. (e, f) The lighter in colour and the longer the bars, the more significant the result is. Significance of data was determined using rank-based ranking; only the top 10 results are shown in each case.

Fig. 2: Protective effects of propionate against LPS-induced barrier disruption. (a) Assessment of the paracellular permeability of hCMEC/D3 monolayers to 70 kDa FITC-dextran following treatment for 24 h with 1 μM propionate, with or without inclusion of 50 ng/ml LPS for the last 12 h of incubation; data are mean ± SEM, n = 3 independent experiments. (b) Trans-endothelial electrical resistance of hCMEC/D3

monolayers following treatment for 24 h with 1 μM propionate, with or without inclusion of 50 ng/ml LPS for the last 12 h of incubation; data are mean ± SEM, *n* = 3 independent experiments. (c) Confocal microscopic analysis of expression of the tight junction components claudin-5, occludin and zona occludens-1 (ZO-1) in hCMEC/D3 cells following treatment for 24 h with 1 μM propionate, with or without inclusion of 50 ng/ml LPS for the last 12 h of incubation. Scale bar (10 μm) applies to all images. Images are representative of at least three independent experiments. (d) Expression of *CD14* mRNA in control and propionate-treated (1 μM; 24 h) hCMEC/D3 cells according to microarray data (data are mean ± SEM, *n* = 3). (e) Surface expression of CD14 protein on control and propionate-treated hCMEC/D3 cells (grey line, unstained cells, black line secondary antibody control, red line FFAR3), data are representative of three independent experiments. (f) Median fluorescence intensity of surface expression of CD14 protein on control and propionate-treated hCMEC/D3 cells, dashed line indicates isotype control fluorescence intensity; data are mean ± SEM, *n*=3 independent experiments.

Fig. 3: Protective effects of propionate against oxidative stress. (a) Representation of stress-response genes significantly upregulated in the current study and directly influenced by NFE2L2, 'the master regulator of antioxidant responses' (Gorrini *et al*, 2013). (b) Confocal microscopic analysis of expression of NFE2L2 (Nrf2) in hCMEC/D3 cells following treatment for 24 h with 1 μM propionate; scale bar (10 μm) applies to all images. Images are representative of at least three independent experiments. (d) Rate of production of reactive oxygen species (ROS) in control and propionate pre-treated (1 μM, 24 h) hCMEC/D3 cells treated for 30 min with the mitochondrial complex I inhibitor rotenone (2.5 μM). Data are mean ± SEM, *n*=3 independent experiments.

Fig. 4: Production of propionate by the human gut microbiota. Propionate can be produced directly or indirectly by cross-feeding from succinate- and lactate-producers (e.g. *Selenomonas*, *Megasphaera* and *Veillonella* spp.). Image produced using information taken from (Reichardt *et al*, 2014). **Akkermansia muciniphila* is known to produce propionate; it is thought to do this via the succinate pathway (Reichardt *et al*, 2014).

Expanded View Fig. 1: Effects of propionate upon expression and activity of typical cerebromicrovascular efflux transporter systems. (a) Surface expression of BCRP, LRP-1 and P-glycoprotein on control and propionate-treated (1 μM, 24 h) hCMEC/D3 cells (black, control, red, propionate), data are representative of three independent experiments. (b) Median fluorescence intensity of surface expression of BCRP, LRP-1 and P-glycoprotein on control and propionate-treated (1 μM, 24 h) hCMEC/D3 cells; data are mean ± SEM, *n*=3 independent experiments. (c) Lack of stimulatory effect of propionate upon BCRP, data are mean ± SEM, *n* = 4. (d) Lack of inhibitory effect of propionate upon stimulated ATP-dependent activity of BCRP, data are mean ± SEM, *n* = 4. (e) Lack of stimulatory effect of propionate upon P-glycoprotein, data are mean ± SEM, *n* = 4. (f) Lack of inhibitory effect of propionate upon stimulated ATP-dependent activity of P-glycoprotein, data are mean ± SEM, *n* = 4.

Fig. 1

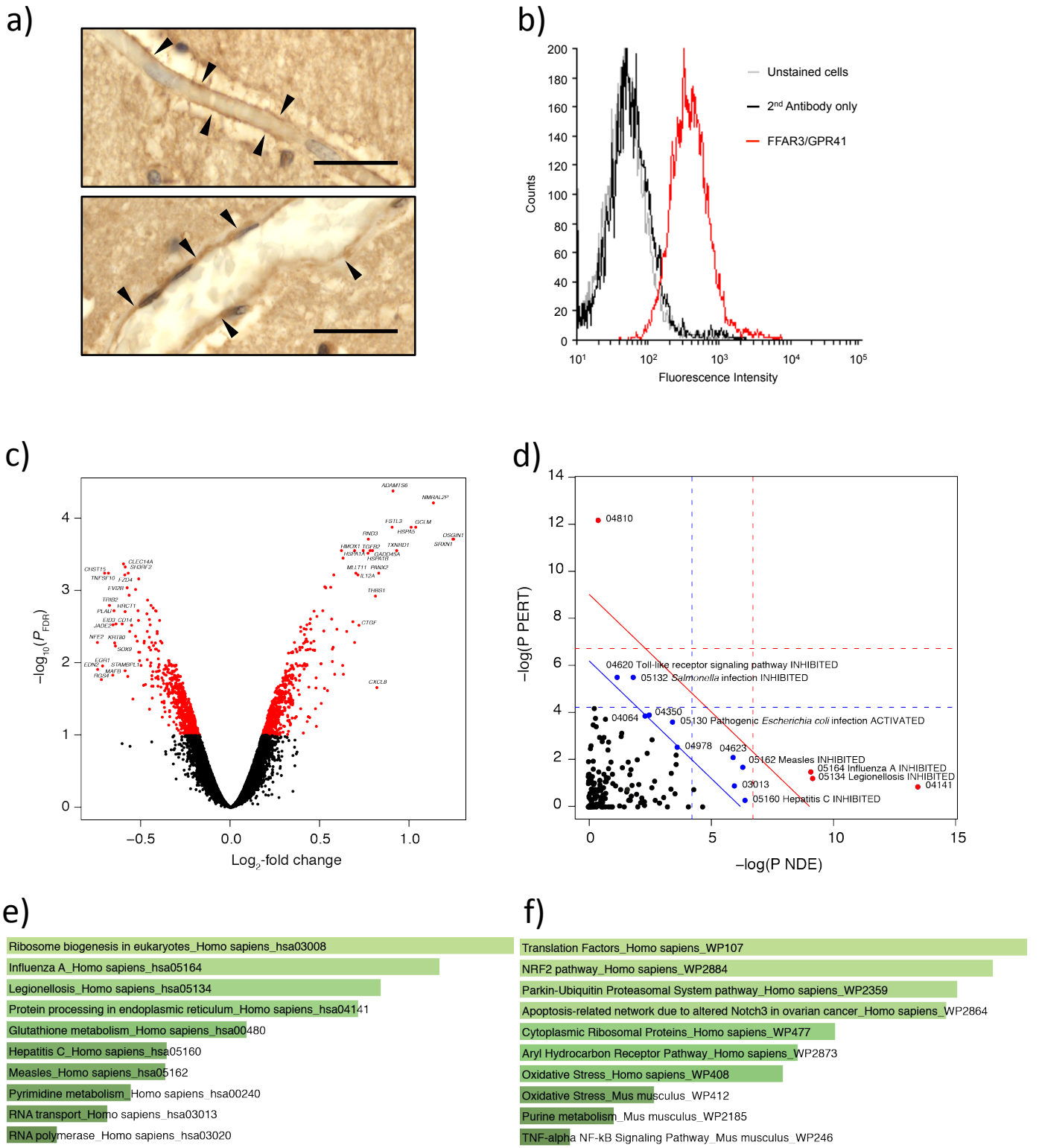
a)
b)
Counts
Fluorescence Intensity
Unstained cells
2nd Antibody only
FFAR3/GPR41
c)
−log10(PFDR)
Log2-fold change
d)
−log(P PERT)
−log(P NDE)
04810
04620 Toll-like receptor signaling pathway INHIBITED
05132 Salmonella infection INHIBITED
04064
04350
05130 Pathogenic Escherichia coli infection ACTIVATED
04978
04623
05162 Measles INHIBITED
05164 Influenza A INHIBITED
05134 Legionellosis INHIBITED
04141
03013
05160 Hepatitis C INHIBITED
e)
Ribosome biogenesis in eukaryotes_Homo sapiens_hsa03008
Influenza A_Homo sapiens_hsa05164
Legionellosis_Homo sapiens_hsa05134
Protein processing in endoplasmic reticulum_Homo sapiens_hsa04141
Glutathione metabolism_Homo sapiens_hsa00480
Hepatitis C_Homo sapiens_hsa05160
Measles_Homo sapiens_hsa05162
Pyrimidine metabolism_Homo sapiens_hsa00240
RNA transport_Homo sapiens_hsa03013
RNA polymerase_Homo sapiens_hsa03020
f)
Translation Factors_Homo sapiens_WP107
NRF2 pathway_Homo sapiens_WP2884
Parkin-Ubiquitin Proteasomal System pathway_Homo sapiens_WP2359
Apoptosis-related network due to altered Notch3 in ovarian cancer_Homo sapiens_WP2864
Cytoplasmic Ribosomal Proteins_Homo sapiens_WP477
Aryl Hydrocarbon Receptor Pathway_Homo sapiens_WP2873
Oxidative Stress_Homo sapiens_WP408
Oxidative Stress_Mus musculus_WP412
Purine metabolism_Mus musculus_WP2185
TNF-alpha NF-kB Signaling Pathway_Mus musculus_WP246

Fig. 2

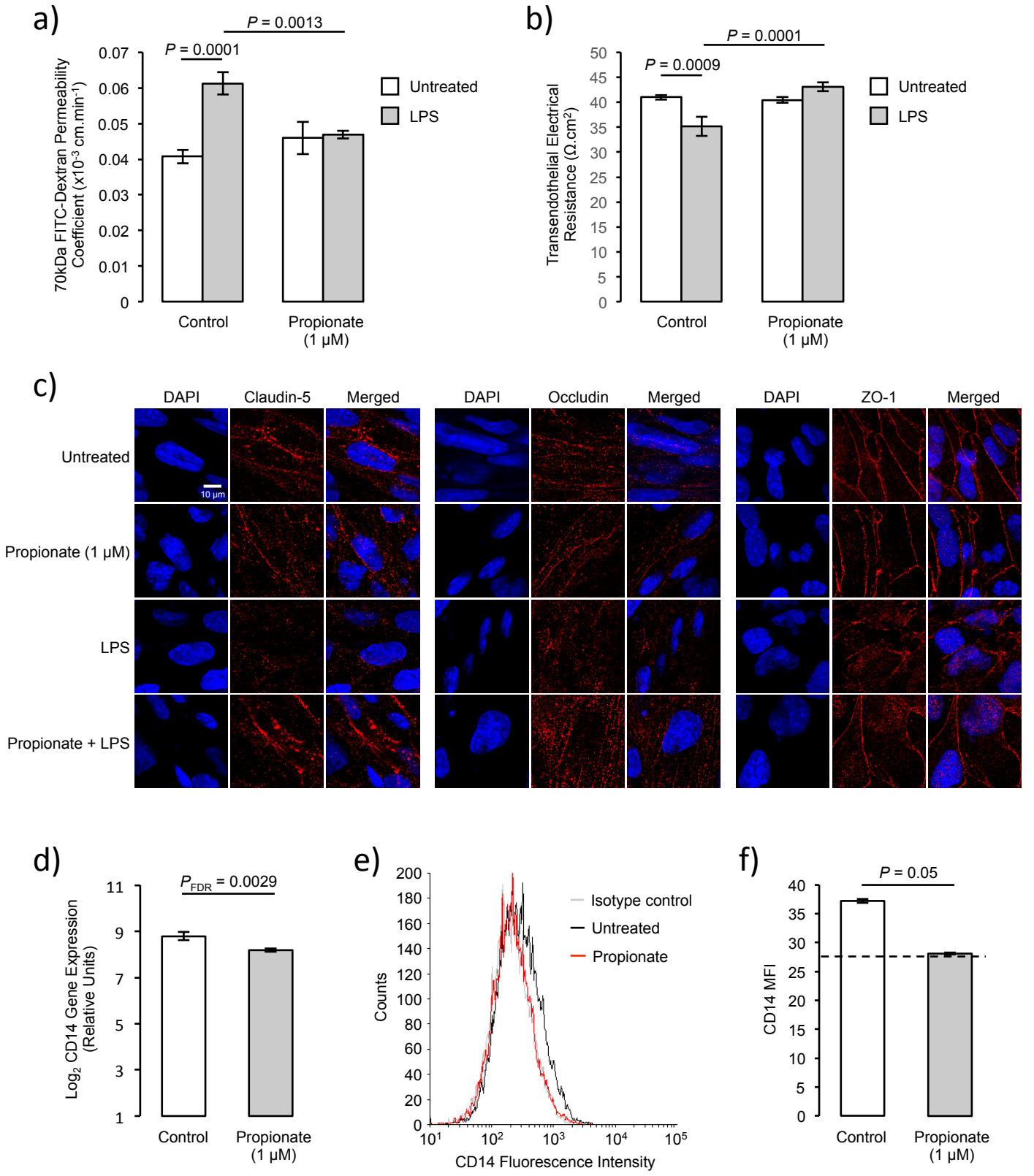
a)
P = 0.0013
P = 0.0001
70kDa FITC-Dextran Permeability Coefficient (x10-3 cm.min-1)
0.07
0.06
0.05
0.04
0.03
0.02
0.01
0
Untreated
LPS
Control
Propionate (1 μM)
b)
P = 0.0001
P = 0.0009
Transendothelial Electrical Resistance (Ω.cm2)
50
45
40
35
30
25
20
15
10
5
0
Untreated
LPS
Control
Propionate (1 μM)
c)
DAPI
Claudin-5
Merged
DAPI
Occludin
Merged
DAPI
ZO-1
Merged
Untreated
Propionate (1 μM)
LPS
Propionate + LPS
10 μm
d)
PFDR = 0.0029
Log2 CD14 Gene Expression (Relative Units)
11
9
7
5
3
1
Control
Propionate (1 μM)
e)
Counts
200
180
160
140
120
100
80
60
40
20
0
Isotype control
Untreated
Propionate
10¹
10²
10³
10⁴
10⁵
CD14 Fluorescence Intensity
f)
P = 0.05
CD14 MFI
40
35
30
25
20
15
10
5
0
Control
Propionate (1 μM)

Fig. 3

a)

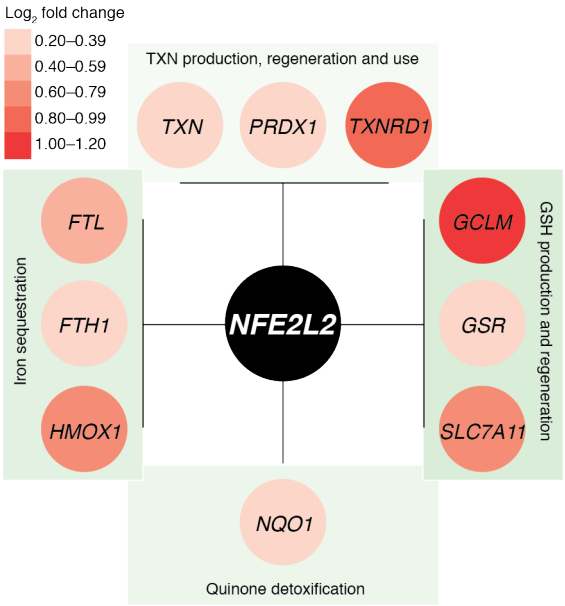
Log2 fold change
0.20–0.39
0.40–0.59
0.60–0.79
0.80–0.99
1.00–1.20
TXN production, regeneration and use
TXN
PRDX1
TXNRD1
Iron sequestration
FTL
FTH1
HMOX1
NFE2L2
GSH production and regeneration
GCLM
GSR
SLC7A11
NQO1
Quinone detoxification

b)

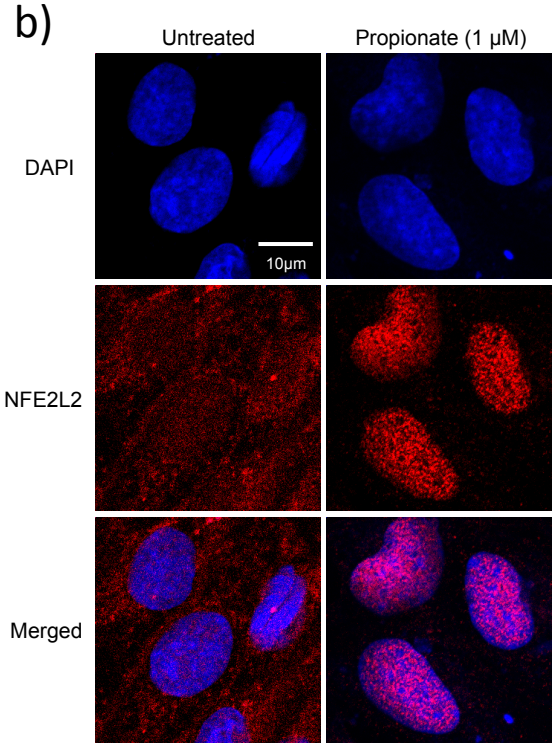
Untreated
Propionate (1 μM)
DAPI
NFE2L2
Merged
10μm

c)

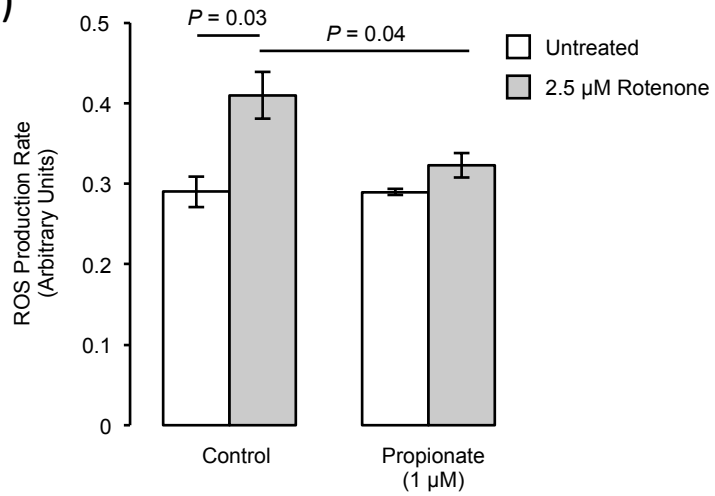
P = 0.03
P = 0.04
Untreated
2.5 μM Rotenone
ROS Production Rate
(Arbitrary Units)
0.5
0.4
0.3
0.2
0.1
0
Control
Propionate
(1 μM)

Fig. 4

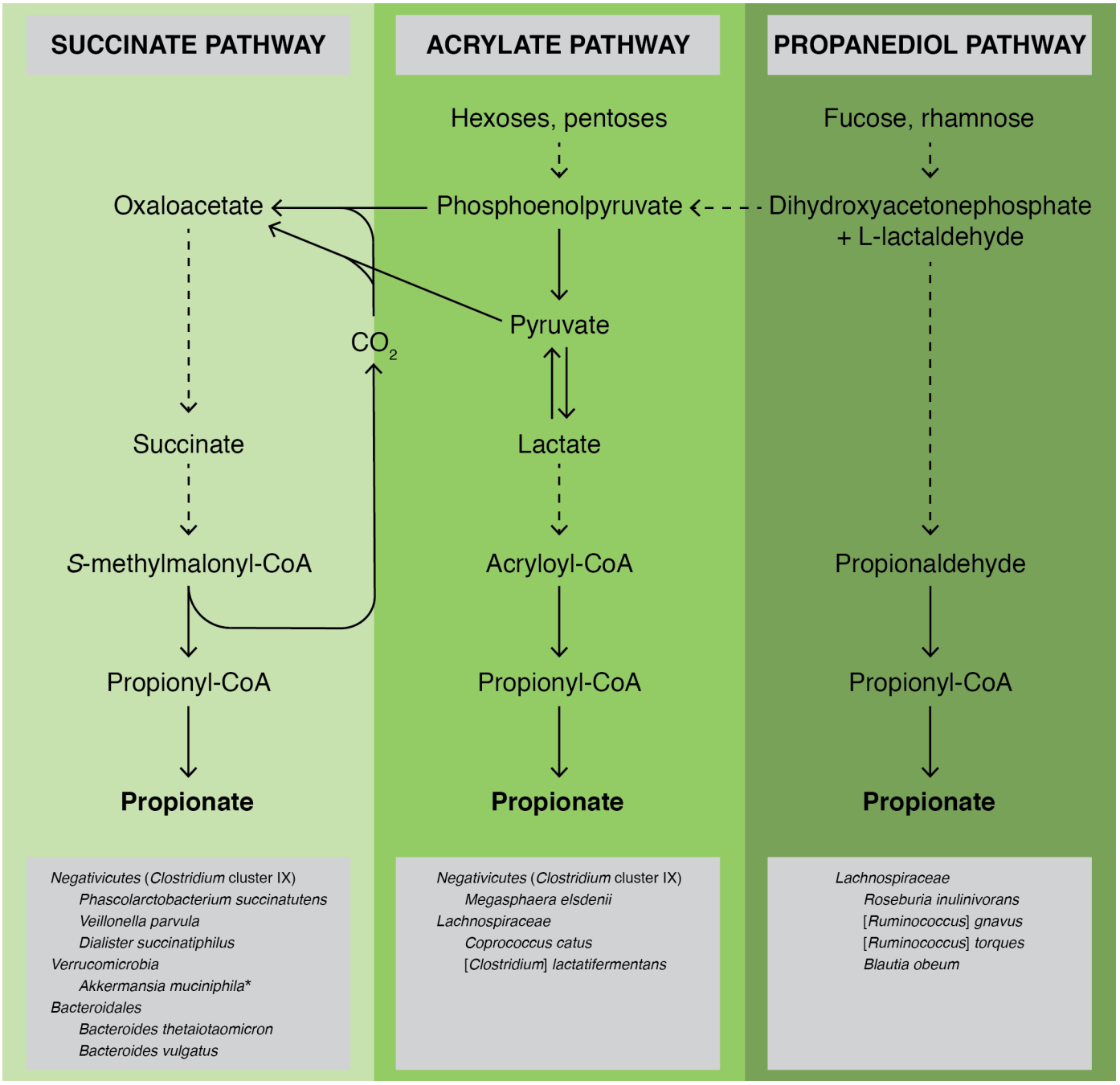
SUCCINATE PATHWAY
ACRYLATE PATHWAY
PROPANEDIOL PATHWAY
Hexoses, pentoses
Fucose, rhamnose
Oxaloacetate
Phosphoenolpyruvate
Dihydroxyacetonephosphate
+ L-lactaldehyde
Pyruvate
CO_2
Succinate
Lactate
S-methylmalonyl-CoA
Acryloyl-CoA
Propionaldehyde
Propionyl-CoA
Propionyl-CoA
Propionyl-CoA
Propionate
Propionate
Propionate
Negativicutes (*Clostridium* cluster IX)
Phascolarctobacterium succinatutens
Veillonella parvula
Dialister succinatiphilus
Verrucomicrobia
*Akkermansia muciniphila**
Bacteroidales
Bacteroides thetaiotaomicron
Bacteroides vulgatus
Negativicutes (*Clostridium* cluster IX)
Megasphaera elsdenii
Lachnospiraceae
Coprococcus catus
[*Clostridium*] *lactatifermentans*
Lachnospiraceae
Roseburia inulinivorans
[*Ruminococcus*] *gnavus*
[*Ruminococcus*] *torques*
Blautia obeum
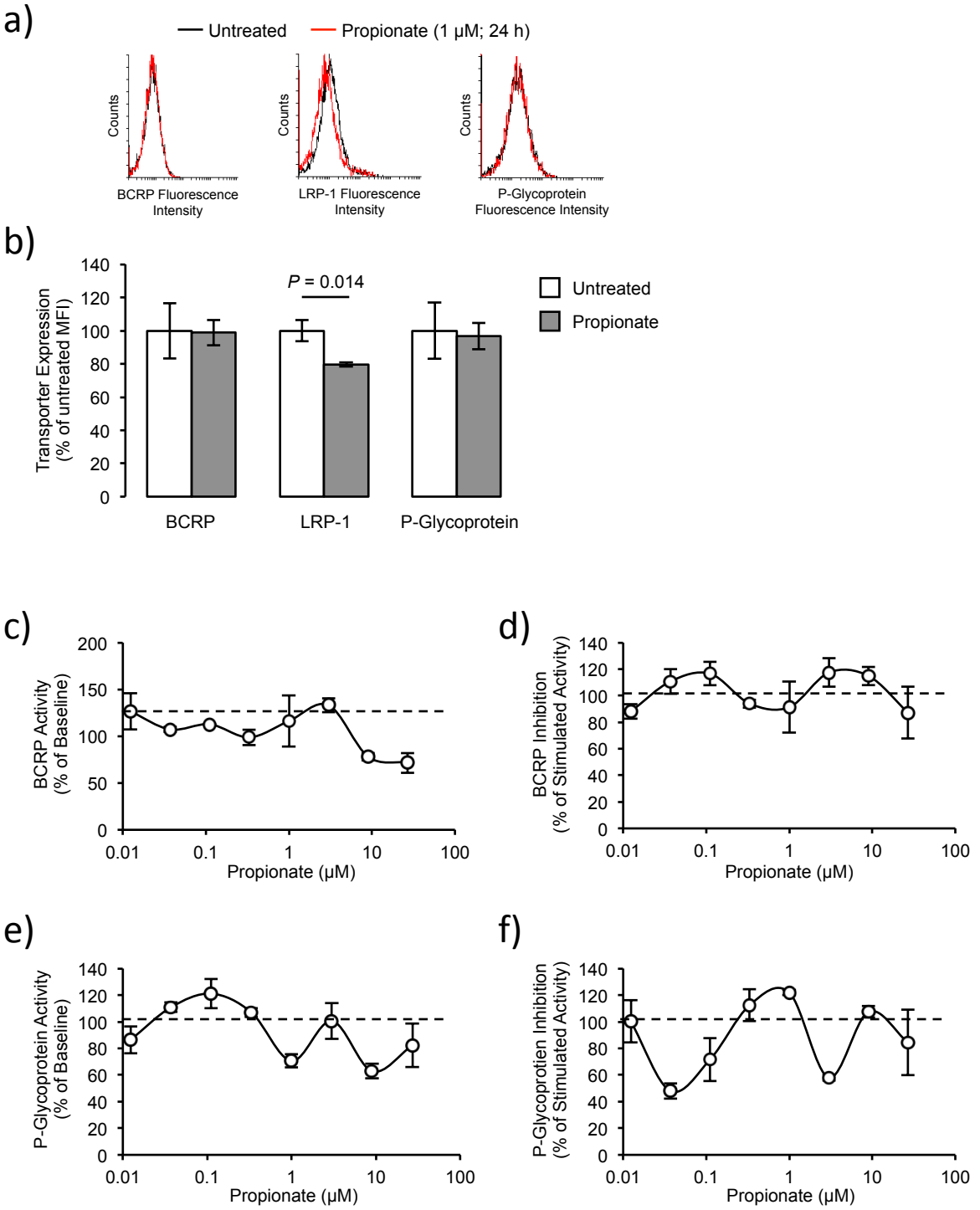
Supplementary Expanded View Fig. 1